ISSN 1936-878X/09/$36.00
PUBLISHED BY ELSEVIER INC.
DOI:10.1016/j.jcmg.2009.04.015

In Vivo Detection of Embryonic Stem Cell–Derived Cardiovascular Progenitor Cells Using Cy3-Labeled Gadofluorine M in Murine Myocardium

Eric D. Adler, MD,* Anne Bystrup, BA,* Karen C. Briley-Saebo, PhD,* Venkatesh Mani, PhD,* Wilson Young, MD, PhD,* Steven Giovanonne, MD,† Perry Altman, BA,* Steven J. Kattman, PhD,‡ Joseph A. Frank, MS, MD,§ Hans J. Weinmann, PhD,‖ Gordon M. Keller, PhD,‡ Zahi A. Fayad, PhD*

New York, New York; Toronto, Ontario, Canada; Bethesda, Maryland; and Berlin, Germany

OBJECTIVES The aim of the current study is to test the ability to label and detect murine embryonic stem cell–derived cardiovascular progenitor cells (ES-CPC) with cardiac magnetic resonance (CMR) using the novel contrast agent Gadofluorine M-Cy3 (GdFM-Cy3).

BACKGROUND Cell therapy shows great promise for the treatment of cardiovascular disease. An important limitation to previous clinical studies is the inability to accurately identify transplanted cells. GdFM-Cy3 is a lipophilic paramagnetic contrast agent that contains a perfluorinated side chain and an amphiphilic character that allows for micelle formation in an aqueous solution. Previous studies reported that it is easily taken up and stored within the cytosol of mesenchymal stem cells, thereby allowing for paramagnetic cell labeling. Investigators in our laboratory have recently developed techniques for the robust generation of ES-CPC. We reasoned that GdFM-Cy3 would be a promising agent for the in vivo detection of these cells after cardiac cell transplantation.

METHODS ES-CPC were labeled with GdFM-Cy3 by incubation. In vitro studies were performed to assess the impact of GdFM-Cy3 on cell function and survival. A total of 500,000 GdFM-Cy3–labeled ES-CPC or control ES-CPC were injected into the myocardium of mice with and without myocardial infarction. Mice were imaged (9.4-T) before and over a 2-week time interval after stem cell transplantation. Mice were then euthanized, and their hearts were sectioned for fluorescence microscopy.

RESULTS In vitro studies demonstrated that GdFM-Cy3 was easily transfectable, nontoxic, stayed within cells after labeling, and could be visualized using CMR and fluorescence microscopy. In vivo studies confirmed the efficacy of the agent for the detection of cells transplanted into the hearts of mice after myocardial infarction. A correspondence between CMR and histology was observed.

CONCLUSIONS The results of the current study suggest that it is possible to identify and potentially track GdFM-Cy3–labeled ES-CPC in murine infarct models via CMR. (J Am Coll Cardiol Img 2009;2:1114–22) © 2009 by the American College of Cardiology Foundation

From the *Cardiovascular Institute and Department of Medicine, Mount Sinai School of Medicine, New York, New York; †Department of Medicine, New York University School of Medicine, New York, New York; ‡McEwen Centre for Regenerative Medicine, University Health Network, Toronto, Ontario, Canada; §National Institutes of Health, Bethesda, Maryland; and ‖Schering AG, Berlin, Germany. Partial support was provided by NIH/NHLBI RO1 HL71021 and NIH/ NHLBI HL78667 grants to Dr. Fayad. Dr. Weinmann works for Schering AG. Drs. Adler and Bystrup contributed equally to this work.

Manuscript received February 1, 2009; revised manuscript received March 31, 2009, accepted April 6, 2009.

Replacement of injured tissue using transplanted exogenous cells has shown therapeutic promise in a wide array of conditions, including spinal cord injury (1), diabetes mellitus (2,3), stroke (4), and cardiovascular disease (5,6). An important limitation to previous clinical studies is the inability to accurately identify transplanted cells. Recent work by our laboratory has resulted in the identification of embryonic stem cell (ES)-derived cardiovascular progenitor cells (ES-CPC) (7), which we speculate would be promising agents for cell therapy. Given that the mechanism

See page 1123

and efficacy of cardiac cell therapy remains uncertain, developing techniques for tracking transplanted cells within the myocardium would be particularly useful.

Thus far, cardiac magnetic resonance (CMR) has been a principal diagnostic modality for cell identification post-transplantation (8,9). Cell identification has been facilitated largely through the use of magnetic resonance (MR) contrast agents that are sensitive, nontoxic, and remain within cells after transplant (10). The 2 classes of MR contrast agents most widely used are iron oxides and gadolinium chelates. Superparamagnetic iron oxide nanoparticles (SPION) have been used across a broad spectrum of cell-labeling applications (11–15). Although iron-labeled cells are highly effective in generating MR signal loss, it is often difficult to differentiate the signal loss generated by iron-laden cells from endogenous sources of signal attenuation (13–16). Gadolinium chelates differ from SPION in their ability to generate increased MR signal intensity when T1-weighted sequences are employed. Most agents are hydrophilic and have difficulty traversing cell membranes. The most widely used is gadopentetate dimeglumine (Gd-DTPA), which can be used for noninvasive angiography and to identify areas of perfusion deficit in the myocardium post-infarct (17–19).

Unlike Gd-DTPA, Gadofluorine M (GdFM) contains a perfluorinated side chain and an amphiphilic character, resulting in micelle formation in an aqueous solution. Its longitudinal relaxivity (r1) is approximately 6 times greater than that of Gd-DTPA chelates and more than twice that of other reported micelle and liposomal formulations (20). In preliminary studies, mesenchymal stem cells labeled by GdFM were identified after injection into the brain of rats using CMR (21). GdFM has also been used in pre-clinical imaging studies of lymphatic tumor metastasis (22), characterization of atherosclerotic plaques (23,24), characterization of mammary tumors (25), assessment of nerve degeneration (26), and labeling human monocytes in vitro (27).

In the present study, we demonstrate the ability to identify transplanted cells in the murine heart using GdFM with a perfluorinated Cy3 side chain (GdFM-Cy3). In vitro studies demonstrated that GdFM-Cy3 was easily transfectable, nontoxic, stayed within cells after labeling, and could be visualized using CMR and fluorescence microscopy. In vivo studies confirmed the efficacy of the agent for the detection of cells transplanted into the hearts of mice with or without myocardial infarction. These findings indicate that GdFM-Cy3 is a promising agent for CMR-based cell-tracking studies.

ABBREVIATIONS AND ACRONYMS

CHESS = chemical shift selective suppression
CNR = contrast-to-noise ratio
CPC = cardiovascular progenitor cell
ES = embryonic stem cell
Gd-DTPA = gadopentetate dimeglumine
GdFM = Gadofluorine M
GdFM-Cy3 = Gadofluorine M-Cy3
ICP-MS = inductively coupled plasma mass spectrometry
SNR = signal-to-noise ratio
TE = time of excitation
TR = time of relaxation

METHODS

Generation and in vitro analysis of embryonic stem cell cardiovascular progenitor cells labeled with GdFM-Cy3. Murine ES cells from a CCE ES line (28) constitutively expressing green fluorescence protein (CCE-GFP) were maintained in serum-free medium supplemented with 1% LIF, glutamine, and BMP4, were expanded on gelatinized culture plates until confluent, and then differentiated in the presence of serum. Flk+ cells were isolated using fluorescence-activated cell sorting (FACS) 4 days after differentiation and cultured in SP-34 serum-free medium supplemented with the cytokines Dickopf, vascular endothelial growth factor, and fibroblast growth factor. GdFM-Cy3 (5 mm) (Schering, Berlin, Germany), prepared as previously published (19), was added to the culture on the 6th day of differentiation. Twelve hours after adding GdFM-Cy3, cells were washed and placed back in serum-free medium in the absence of GdFM-Cy3.

ES-CPC were kept in culture over a 14-day period and periodically harvested. Inductively coupled plasma mass spectrometry (ICP-MS) was performed, and the concentration of GdFM-Cy3 per cell was calculated. To determine whether GdFM-Cy3 caused cell death, a colorimetric assay was performed as originally described by Mosmann (29). To further assess for apoptosis after extended exposure to GdFM-Cy3, cells were analyzed using

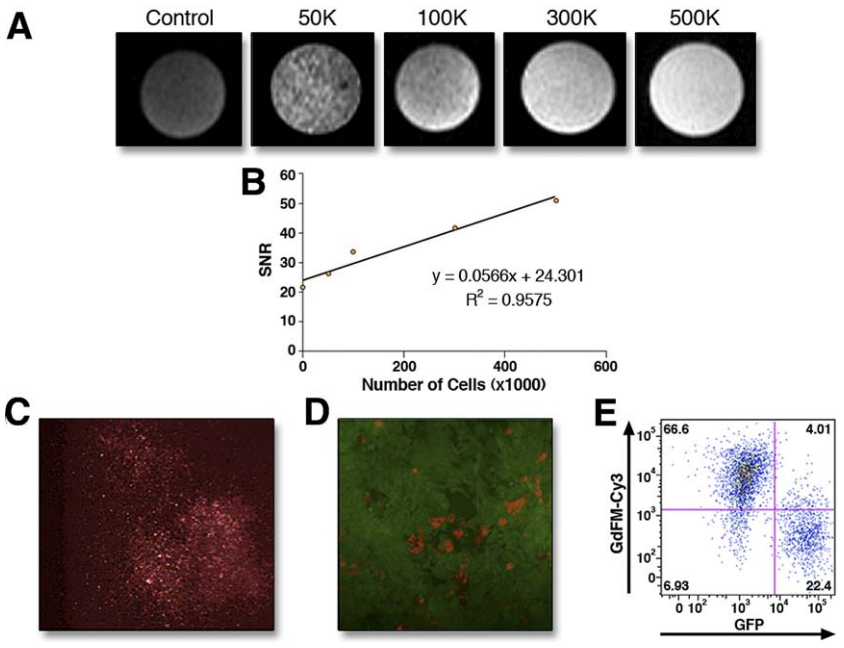

Figure 1. In Vitro Analysis of Cells Labeled With GdFM-Cy3

(A) Agarose gels containing 500,000 unlabeled, or 50,000, 100,000, 300,000, or 500,000 GdFM-Cy3–labeled cells were imaged with 9.4-T cardiac magnetic resonance. **(B)** A linear relationship between signal-to-noise ratio (SNR) and cell number was observed. **(C)** Cells labeled with gadofluorine M-Cy3 (GdFM-Cy3) imaged using fluorescence microscopy. **(D and E)** GdFM-Cy3–labeled cells coplated with embryonic stem cells constitutively expressing green fluorescence protein (GFP). Fluorescence microscopy demonstrated that Cy3 cells were not GFP positive **(D)**. Flow cytometry performed 48 h after coplating the cells demonstrated 2 major populations, a GdFM-Cy3–positive population and a GFP-positive population **(E)**. Also see accompanying Online Video 1.

a commercially available kit for the apoptosis-specific phospholipid binding protein Annexin V (BD Pharmingen, Franklin Lakes, New Jersey).

To evaluate whether GdFM-Cy3 can travel from labeled cells into neighboring unlabeled cells, a population of cells labeled with GdFM-Cy3 were combined with an equal number of ES-CPC from a line that constitutively expressed GFP. Flow cytometry was performed 48 h later to assess for the presence of GFP-positive Cy3-positive cells, indicating the spread of GdFM-Cy3 into unlabeled cells.

Cell transplantation. Cell injection was performed in severe combined immune deficiency (SCID) beige mice, deficient in B, T, and NK cells. The hearts of 4-month-old female SCID beige mice (Jackson Laboratories, Bar Harbor, Maine) were injected with either ES-CPC labeled with GdFM-Cy3 (n = 4) or unlabeled ES-CPC (n = 4). Cells were injected directly into the myocardium in a volume of 7.5 μl. A total of 500,000 cells were used per injection, and 1 injection was performed per mouse. No mortality was observed as a result of cell transplant. These experiments were then repeated in mice with myocardial infarction using a coronary ligation model. After coronary ligation, intramyocardial injection was performed using labeled ES-CPC (n = 5) or unlabeled cells (n = 6). Three mice died within 1 week of the post-operative period. Two died immediately after surgery (1 from the cell treatment group and 1 from the unlabeled cell group), and 1 was found dead 24 h after surgery (from the unlabeled cell group). This mortality rate is consistent with the mortality rate of this surgery in our laboratory's experience. This resulted in a total of 4 infarcted mice from each surviving group.

In vitro CMR. To test the ability of CMR to detect GdFM-Cy3–labeled ES-CPC, agarose gels containing labeled or unlabeled cells were imaged on a 9.4-T dedicated mouse CMR scanner (Bruker Instruments, Billerica, Massachusetts) equipped with a 89-mm bore system operating at a proton frequency of 400 MHz. All samples were prepared by adding 0.2 ml of warm agarose gel to 1-ml tubes containing 500,000, 300,000, 100,000, and 50,000 labeled ES-CPC.

In vivo imaging of infarcted mice. The in vivo detection of GdFM-Cy3–labeled ES-CPC was performed using a 9.4-T dedicated mouse CMR scanner (Bruker Instruments) equipped with a 89-mm

bore system operating at a proton frequency of 400 MHz. To identify and track the labeled cells over time, mice were imaged prior to transplantation, as well as 1, 7, and 14 days post-transplant. The longitudinal- and short-axis cine views of the heart were localized using scout scans in different planes. Multiple images (n = 10) throughout the cardiac cycle resulted in the formation of a video that allowed for the identification of GdFM-Cy3–labeled cells moving within the myocardial wall. The ability to follow the signal within the moving myocardium allowed for the identification of the labeled cells relative to coronary vessels that may also generate a positive signal on the T1-weighted sequence used.

MR images were analyzed by calculating the contrast-to-noise ratios (CNR) of hyperintense regions (containing the GdFM-Cy3 ES-CPC) and areas of normal myocardium (relative to the standard deviation of the noise). CNR analysis was performed using 4 mice from each group. Analysis was performed in control mice (unlabeled ES-CPC) 2 weeks after injection, and in labeled mice (GdFM-Cy3–labeled cells) 1, 7, and 14 days post-injection. Analysis was performed on both infarcted and noninfarcted animals, and the CNR between GdFM-Cy3–positive areas versus areas of the surrounding myocardium were determined. The CNR for each group is presented as mean ± SD. The region of interest (ROI) size was kept constant at 0.06 mm^2 for each group. The statistical significance of comparisons between all groups was determined using ANOVA analysis with a Tukey-Kramer multiple comparison post-test.

Histology. Fluorescent immunohistochemistry was used for the detection and characterization of the transplanted GdFM-Cy3–labeled cells. Myocytes were identified using anti-mouse cTnT (Chemicon, Temicula, California) and anti-alpha-actinin (Sigma-Aldrich) was used to identify myocytes in conjunction with the goat anti-mouse IgG alexa fluor 488 antibody (Invitrogen, Carlsbad, California). DAPI (Vectorlabs, Burlingame, California) was used to stain all cell nuclei (blue).

RESULTS

Isolation of ES-CPC and incubation with GdFM-Cy3. Five days after plating the Flk+ population, synchronous waves of contracting cells could be identified across the entire plate and remained beating throughout the study period. FACS analysis demonstrated that over 60% of cells expressed cardiac-specific troponin T (Online Fig. 1). Twelve hours after labeling of GdFM-Cy3, red fluorescent cells were seen using a fluorescence microscope (Fig. 1C) (Online Video 1). ICP-MS revealed that 91% of the GdFM-Cy3 added to the ES-CPC was taken up by the cells.

CMR was performed on cell agarose gel phantoms containing 500,000, 300,000, 100,000, and 50,000 cells. The SNR values reflect the MR signal obtained for the number of cells homogeneously distributed into a 0.2-ml volume. Given that the inner diameter of the tubes used to construct the phantoms was 5 mm and since each slice was 0.5-mm thick, the total number of cells in any given

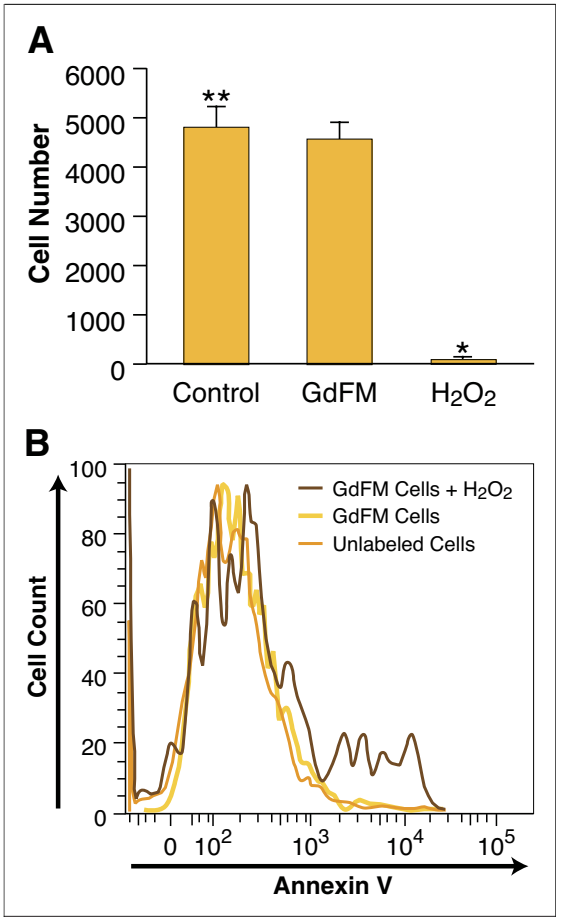

Figure 2. GdFM-Cy3 Toxicity Assays

(A) MTT assay. After 24 h, there was no difference in the number of live cells in both GdFM-Cy3–labeled and unlabeled populations of cardiovascular progenitor cells. *p > 0.001 vs. control and GdFM; **p > 0.05 control and GdFM. **(B)** Annexin V expression measured using flow cytometry. There was no difference in the expression of Annexin V in labeled and unlabeled populations, whereas 16% of cells exposed to H_2O_2 for 2 h expressed Annexin V. Abbreviation as in Figure 1.

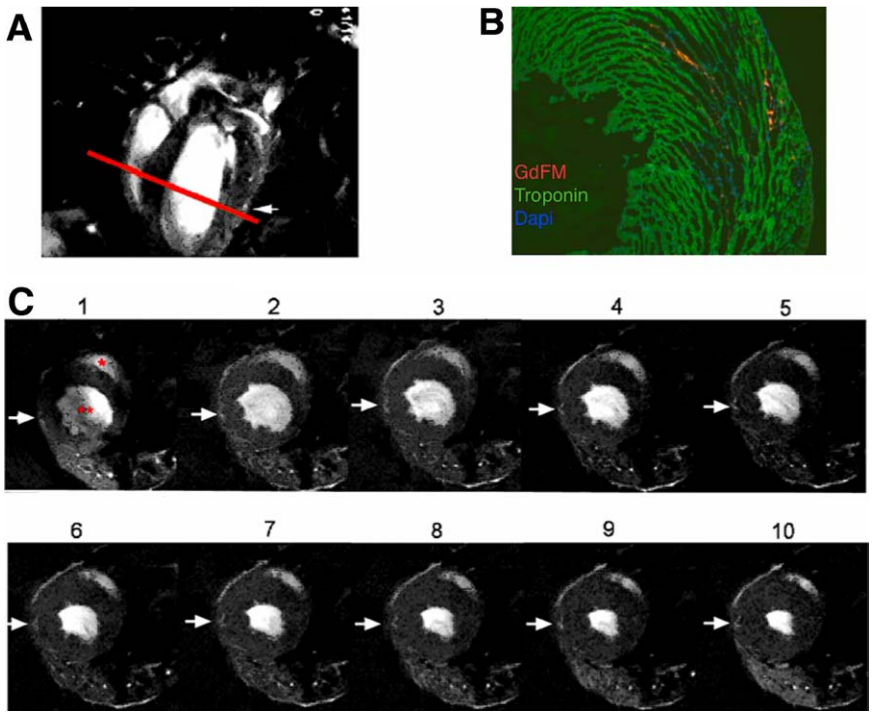

Figure 3. Evaluation of Noninfarcted Mice

T1-weighted high-resolution cardiac magnetic resonance (CMR) scan of noninfarcted mouse 1 day after injection **(A)**. Longitudinal image indicating position of axial slice **(red line)** in top frame. **(B)** Corresponding histology shows GdFM-Cy3 **(red)** within the myocardial wall, cardiac Troponin T stain **(green)**, and DAPI **(blue)**, 5×. **(C)** Frames 1 through 10 depict different frames within cardiac cycle. **Red** * indicates the right ventricle and **red** ** indicates the left ventricle. **Arrows** show volume containing GdFM-Cy3 cells. Abbreviation as in Figure 1.

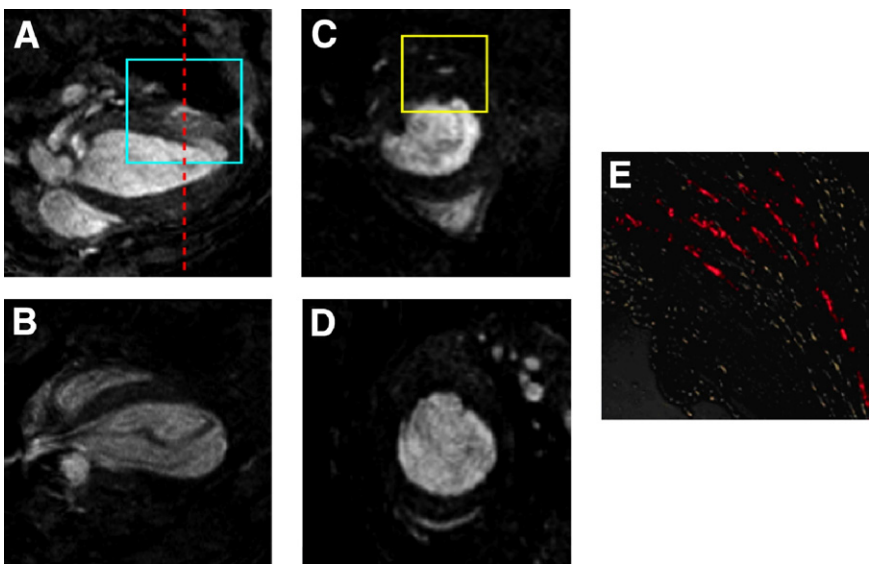

Figure 4. Evaluation of Infarcted Mice

(A to D) A 9.4-T CMR was performed 1 day post-transplantation on mice injected with embryonic stem cell-cardiovascular progenitor cells (ES-CPC) labeled with GdFM-Cy3 (**A**: long axis and **C**: short axis; **red dotted line** corresponds to location of short-axis image) or unlabeled ES-CPC (**B**: long axis and **D**: short axis). An area of increased signal intensity was seen in short axis **(yellow box, C)**. **(E)** Fluorescent microscopy on frozen cardiac sections. Areas of Cy3-positive cells could be seen corresponding to **blue and yellow boxes** seen in **A and C**, respectively.

0.5mm slice is: 1,250, 750, 250, and 125 for 500,000, 300,000, 100,000, and 50,000 cells, respectively (assumes homogeneous distribution of cells). The results indicate a linear increase in SNR with increasing cell number, as shown in Figure 1A. A total of 125 cells within a slice could be easily identified by this method.

Cells labeled with GdFM-Cy3 were then cocultured with ES-CPC from a line constitutively expressing GFP. After 48 h of coincubation, the majority of cells were labeled with either Cy3 or GFP, with only 4% of cells expressing both markers (Figs. 1D and 1E).

GdFM-Cy3 toxicity was assessed using MTT and Annexin assays. After 12 h of exposure, the MTT assay demonstrated that the viable cell number between treated (4,549 ± 388) and untreated (4,771 ± 447) populations was similar ($p > 0.05$), in comparison to H_2O_2-treated cells (50 ± 68) ($p < 0.001$) (Fig. 2A). Fourteen days after labeling, apoptosis assays were done using Annexin V. No difference in Annexin V was detected between labeled and unlabeled groups (Fig. 2B). In addition, GdFM-Cy3–labeled cells continued to spontaneously contract and were easily identified by fluorescent microscopy (Online Video 1). Thus, we conclude that GdFM-Cy3 does not affect cell survival or function in vitro.

In vivo studies. Positive MR signal enhancement was clearly observed on both long- and short-axis images of the injected hearts. GdFM-Cy3 ES-CPC were identified in mice with and without myocardial infarction, as shown in representative images in Figures 3 and 4. Positive MR signal was noted in 3 to 4 contiguous short-axis images in each animal injected. Signal was detected up to 1 week after transplantation in noninfarcted mice and up to 14 days in infarcted mice, but not in regions containing unlabeled ES-CPC (Figs. 4B and 4D). Figure 5 shows images in a mouse with an infarction obtained 24 h and 14 days after transplantation of GdFM-Cy3–lableled ES-CPC. Signal is clearly seen at both time points, though much more diffuse at the later time point.

To quantify signal enhancement, CNR values were calculated. In mice with myocardial infarctions, CNR values of 0.21 ± 0.01, 1.62 ± 0.51, and 2.81 ± 0.55 were observed in mice injected with unlabeled cells, GdFM-Cy3–labeled cells 1 day post-transplant, and GdFM-Cy3–labeled cells 14 days post-transplant, respectively (Fig. 6). Additionally, the CNR values in noninfarcted mice were 0.27 ± 0.09, 1.67 ± 0.33, and 1.06 ± 0.17 in mice injected with unlabeled cells, mice with GdFM-Cy3–labeled cells after 1 day, and mice with GDFM-Cy3–labeled cells after 14 days, respectively (Fig. 6). The CNR values obtained for all GdFM-Cy3 transplant groups were significantly greater than the values obtained for the unlabeled control groups ($p < 0.001$) at 1 day and 14 days post cell transplant. For the infarcted group, the CNR values increased from day 1 to day 14 by 73% ($p < 0.001$). In noninfarcted mice, no significant increases in CNR values were observed from day 1 to day 14. Instead, a significant decrease in CNR values (36%, $p < 0.001$) was observed. The CNR values obtained 14 days

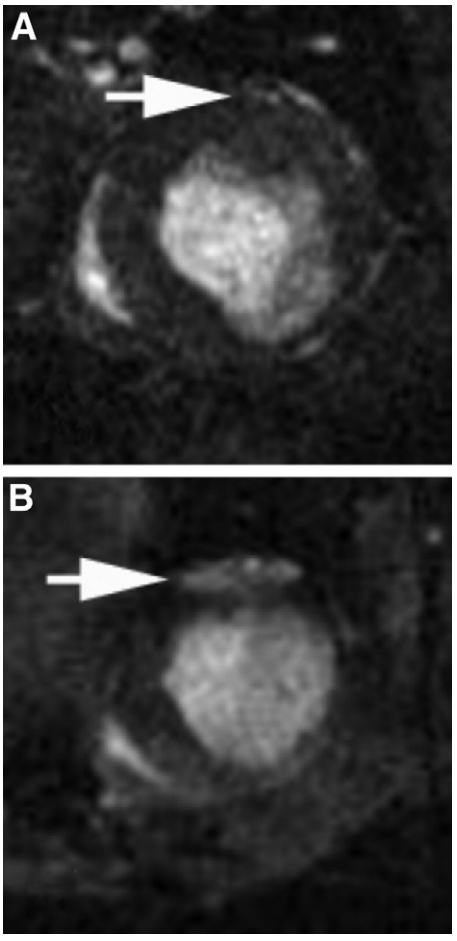

Figure 5. Serial Imaging of GdFM-Cy3–Labeled Cells Over Time

(A) A 9.4-T CMR performed 24 h after the injection of GdFM-Cy3–labeled ES-CPC into a mouse with surgically induced myocardial infarction. **(B)** A 9.4-T CMR performed in the same mouse 14 days after the injection of GdFM-Cy3 ES-CPC. Significant enhancement of the MR signal **(arrows)** in the anterior wall of the left ventricle could be visualized. Abbreviations as in Figures 1 and 3.

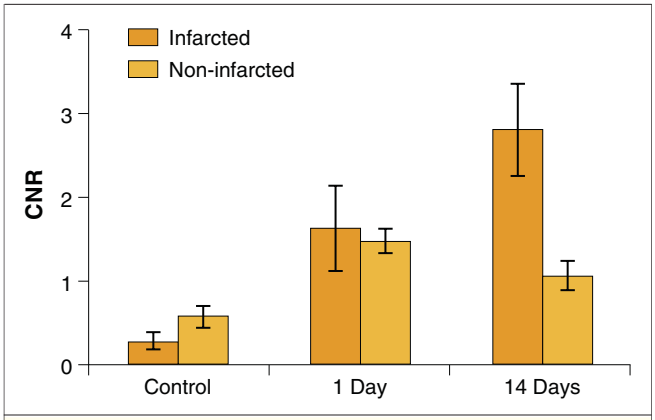

Figure 6. Contrast-to-Noise Ratios

Contrast-to-noise ratios (CNR) calculated from infarcted and noninfarcted mice injected with control (unlabeled cells) scanned at day 14 after injection or injected with GdFM-Cy3–labeled cells and scanned at day 1 and day 14. All comparisons are statistically significant and have a $p < 0.001$, except for infarct day 1 versus noninfarct day 14 ($p < 0.01$), and infarct and noninfarcted day 1 and control ($p > 0.05$).

post-transplant for the infarcted mice were 165% greater than that observed for the noninfarcted group ($p < 0.001$).

Microscopy revealed the presence of GdFM-Cy3–positive cells in sections matching MR signal enhancement, as shown in Figures 3 and 4. Cy3-positive cells stained positive for alpha actinin and GFP, thereby indicating that GdFM-Cy3 was present in the donor ES-CPC cell population (Fig. 7). Cells were found in areas both proximal and within infarcted tissue.

DISCUSSION

The current study demonstrates the potential of GdFM-Cy3 for the detection of transplanted ES-CPC in the mouse myocardium. Phantom imaging using cells in agarose gels demonstrated that it is possible to detect as few as 125 cells per 0.005 mm^3 (Figs. 1A and 1B). The cellular uptake of GdFM-Cy3 was effective (Figs. 1C to 1E), and unlike ferromagnetic agents, did not require the use of transfection agents or other methods to promote labeling. Minimal migration of the MR label was observed between the GdFM-Cy3–labeled cells (in vitro) and GFP-expressing control cells. These results indicate limited cellular excretion and subsequent uptake by neighboring cells within the time period tested. This is critical for cell labels intended for tracking, since cellular excretion/metabolism may dilute the MR signal observed. Previous work has shown that the gadolinium label remains primarily within the cytoplasmic compartment (without uptake into lysosomes and/or endosomes), thereby limiting metabolism and enabling effective MR signal enhancement (as observed both in vitro and in vivo) (22). In vitro work also suggests that ES-CPC may be safely labeled with GdFM-Cy3 without affecting viability, as shown in Figure 2, or contractile function, as shown in Online Video 1.

GdFM-Cy3 ES-CPC were clearly visualized in the myocardium of mice after injection (Fig. 3). A correspondence between the in vivo MR images and ex vivo fluorescence images (for Cy3) was observed in all mice. Given that most cell therapy will be performed in injured hearts, we included a cohort of mice with surgically induced myocardial infarction (Figs. 4 and 5). Fourteen days after injection, no cells were noted by CMR or histology in the noninfarct group. However, in the infarcted mice, MR signal enhancement was observed over the entire 2-week time interval. Fluorescent immunolabeling confirmed that post-transplant, the GdFM-Cy3 remained within transplanted cells (Fig. 7). These findings suggest that the milieu post-infarction may actually be more supportive of cells in the long term than that of the noninfarcted heart.

Quantitative evaluation of the MR data revealed that the CNR values increase from 24 h to 14 days post-transplant. The reduced CNR at early time points is most likely related to T2* effects that may modulate and reduce the MR signal observed. As the cells diffuse or migrate as a function of time, the concentration of the MR label within a given volume is reduced, thereby reducing T2* effects and increasing the MR signal observed.

CONCLUSIONS

GdFM-Cy3 is a novel CMR contrast agent that is easily taken up by ES-CPC in vitro, is retained by these cells, and does not affect cell function or survival. Transplanted cells labeled with GdFM-Cy3 can be identified in vivo and tracked using T1-weighted gradient echo CMR sequences. Although the current work is focused on the myocardium, we believe GdFM-Cy3 may allow for labeling of other cell types, as well as for

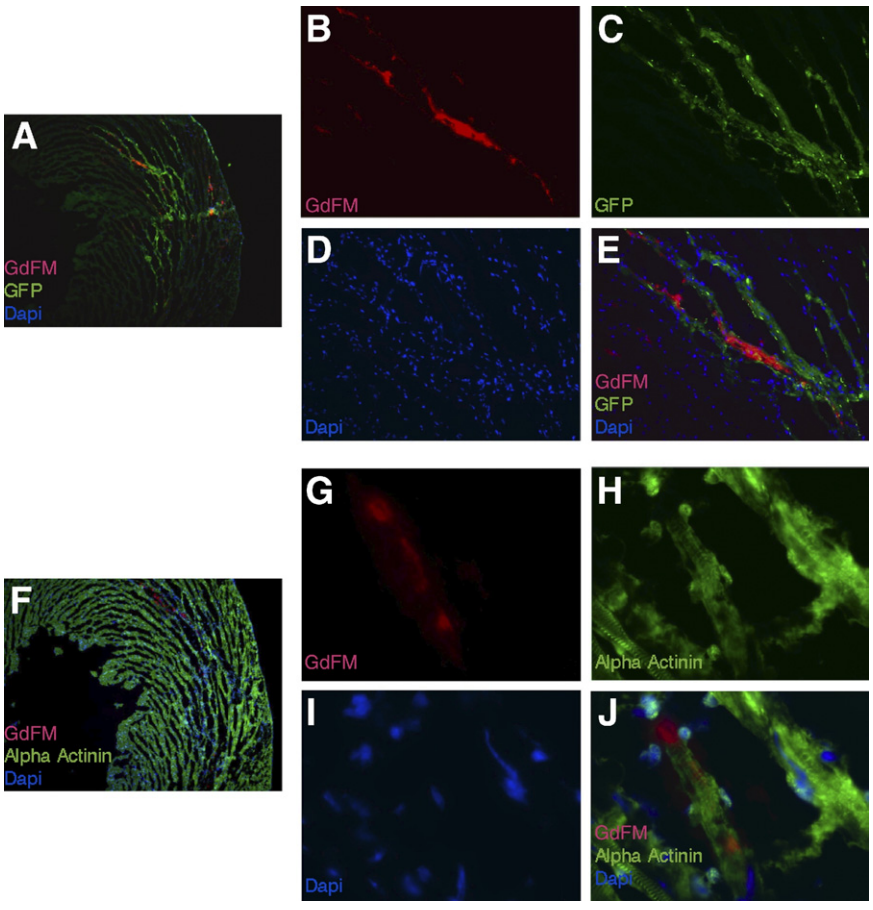

Figure 7. Frozen Sections of Heart Imaged Using Fluorescence Microscopy

(A) A 5× view of section with **red** (GdFM-Cy3), **green** (GFP), and **blue** (DAPI) channels. **(B) Red** channel 20× view demonstrating GdFM-Cy3–positive cells. **(C) Green** channel 20× view demonstrating GFP-positive cells. **(D) Blue** channel 20× view demonstrates DAPI-positive cells. **(E)** Overlap of all 3 channels confirming that GdFM-Cy-3 was within GFP-positive cells. **(F)** A 5× view of section stained with alpha-actinin and alexa 488 secondary antibody **(green)**. **(G) Red** channel 20× view demonstrating GdFM-Cy3–positive cells. **(H) Green** channel 20× view demonstrating alpha-actinin–positive cells. **(I) Blue** channel 20× view demonstrates DAPI-positive cells. **(J)** Overlap of all 3 channels confirming that GdFM-Cy3 was within alpha-actinin–positive cells. Abbreviation as in Figure 1.

transplantation into other organs and organ systems. Future studies will evaluate the ability of the technology to work in larger animals at clinically relevant field strengths and with longer follow-up periods.

Reprint requests and correspondence: Dr. Eric D. Adler, Mount Sinai School of Medicine, 1 Gustave L. Levy Place, Box 1030, New York, New York 10029. *E-mail: eric.adler@mssm.edu.*

REFERENCES

1. Liu S, Qu Y, Stewart TJ, et al. Embryonic stem cells differentiate into oligodendrocytes and myelinate in culture and after spinal cord transplantation. Proc Natl Acad Sci U S A 2000;97:6126–31.
2. Chen LB, Jiang XB, Yang L. Differentiation of rat marrow mesenchymal stem cells into pancreatic islet beta-cells. World J Gastroenterol 2004;10:3016–20.
3. Lumelsky N, Blondel O, Laeng P, Velasco I, Ravin R, McKay R. Differentiation of embryonic stem cells to insulin-secreting structures similar to pancreatic islets. Science 2001;292:1389–94.
4. Shen LH, Li Y, Chen J, et al. Intracarotid transplantation of bone marrow stromal cells increases axon-myelin remodeling after stroke. Neuroscience 2006;137:393–9.
5. Kolossov E, Bostani T, Roell W, et al. Engraftment of engineered ES cell-derived cardiomyocytes but not BM cells restores contractile function to the infarcted myocardium. J Exp Med 2006;203:2315–27.
6. Herreros J, Prosper F, Perez A, et al. Autologous intramyocardial injection of cultured skeletal muscle-derived stem cells in patients with non-acute myocardial infarction. Eur Heart J 2003;24:2012–20.

JACC: CARDIOVASCULAR IMAGING, VOL. 2, NO. 9, 2009
SEPTEMBER 2009:1114–22

7. Kattman SJ, Huber TL, Keller GM. Multipotent flk-1+ cardiovascular progenitor cells give rise to the cardiomyocyte, endothelial, and vascular smooth muscle lineages. Dev Cell 2006;11:723–32.
8. Beeres SL, Bengel FM, Bartunek J, et al. Role of imaging in cardiac stem cell therapy. J Am Coll Cardiol 2007;49:1137–48.
9. Zhou R, Acton PD, Ferrari VA. Imaging stem cells implanted in infarcted myocardium. J Am Coll Cardiol 2006;48:2094–106.
10. Frangioni JV, Hajjar RJ. In vivo tracking of stem cells for clinical trials in cardiovascular disease. Circulation 2004;110:3378–83.
11. Weber R, Wegener S, Ramos-Cabrer P, Wiedermann D, Hoehn M. MRI detection of macrophage activity after experimental stroke in rats: new indicators for late appearance of vascular degradation? Magn Reson Med 2005;54:59–66.
12. Kustermann E, Roell W, Breitbach M, et al. Stem cell implantation in ischemic mouse heart: a high-resolution magnetic resonance imaging investigation. NMR Biomed 2005;18:362–70.
13. Mani V, Adler E, Briley-Saebo KC, et al. Serial in vivo positive contrast MRI of iron oxide-labeled embryonic stem cell-derived cardiac precursor cells in a mouse model of myocardial infarction. Magn Reson Med 2008;60:73–81.
14. Wu YL, Ye Q, Foley LM, et al. In situ labeling of immune cells with iron oxide particles: an approach to detect organ rejection by cellular MRI. Proc Natl Acad Sci U S A 2006;103:1852–7.
15. Tallheden T, Nannmark U, Lorentzon M, et al. In vivo MR imaging of magnetically labeled human embryonic stem cells. Life Sci 2006;79:999–1006.
16. Wegener S, Weber R, Ramos-Cabrer P, et al. Temporal profile of T2-weighted MRI distinguishes between pannecrosis and selective neuronal death after transient focal cerebral ischemia in the rat. J Cereb Blood Flow Metab 2006;26:38–47.
17. Rajagopalan S, Prince M. Magnetic resonance angiographic techniques for the diagnosis of arterial disease. Cardiol Clin 2002;20:501–12, v.
18. Nagel E, Klein C, Paetsch I, et al. Magnetic resonance perfusion measurements for the noninvasive detection of coronary artery disease. Circulation 2003;108:432–7.
19. Kim RJ, Fieno DS, Parrish TB, et al. Relationship of MRI delayed contrast enhancement to irreversible injury, infarct age, and contractile function. Circulation 1999;100:1992–2002.
20. Meding J, Urich M, Licha K, et al. Magnetic resonance imaging of atherosclerosis by targeting extracellular matrix deposition with Gadofluorine M. Contrast Media Mol Imaging 2007;2:120–9.
21. Giesel FL, Stroick M, Griebe M, et al. Gadofluorine M uptake in stem cells as a new magnetic resonance imaging tracking method: an in vitro and in vivo study. Investigative radiology 2006;41:868–73.
22. Misselwitz B, Platzek J, Weinmann HJ. Early MR lymphography with gadofluorine M in rabbits. Radiology 2004;231:682–8.
23. Barkhausen J, Ebert W, Heyer C, Debatin JF, Weinmann HJ. Detection of atherosclerotic plaque with Gadofluorine-enhanced magnetic resonance imaging. Circulation 2003;108:605–9.
24. Sirol M, Itskovich VV, Mani V, et al. Lipid-rich atherosclerotic plaques detected by gadofluorine-enhanced in vivo magnetic resonance imaging. Circulation 2004;109:2890–6.
25. Raatschen HJ, Swain R, Shames DM, et al. MRI tumor characterization using Gd-GlyMe-DOTA-perfluorooctylmannose-conjugate (Gadofluorine M), a protein-avid contrast agent. Contrast Media Mol Imaging 2006;1:113–20.
26. Bendszus M, Wessig C, Schutz A, et al. Assessment of nerve degeneration by gadofluorine M-enhanced magnetic resonance imaging. Ann Neurol 2005;57:388–95.
27. Henning TD, Saborowski O, Golovko D, et al. Cell labeling with the positive MR contrast agent Gadofluorine M. Eur Radiol 2007;17:1226–34.
28. Keller G, Kennedy M, Papayannopoulou T, Wiles MV. Hematopoietic commitment during embryonic stem cells differentiation in culture. Mol Cell Biol 1993;13:473–86.
29. Mosmann T. Rapid colorimetric assay for cellular growth and survival: application to proliferation and cytotoxicity assays. J Immunol Methods 1983;65:55–63.

Key Words: cells ■ cardiac magnetic resonance ■ myocardial infarction.

APPENDIX

For an expanded Methods section, as well as a supplementary figure and video and their legends, please see the online version of this article.